Reprinted from Modeling of Inelastic Behavior
of RC Structures Under Seismic Loads
Committee Report
American Society of Civil Engineers

Analysis of Inelastic Behavior and Failure Modes of Confined Concrete by Elasto-Plastic Softening Model

Hiromichi Yoshikawa[1] and Kazuhiro Yamakawa[2]

Abstract

It has been widely accepted that quasi-brittle materials such as concrete, ceramics and rocks exhibit inelasticity and spatial discontinuities in the form of localization. Many researchers have been involved with this traditional and fascinating work and contributed to much progress in nonlinear analysis and localization detection. To this end, concrete columns laterally confined by reinforcement are analyzed by employing the elasto-plastic constitutive model. Confined concrete in a state of triaxial stresses exhibits compressive failure, sometimes with localization.

The objective of the present paper is to investigate the nonlinear behavior and failure diagnostics of transversely confined concrete. Macroscopic modeling of confined concrete is developed on the stress/strain level by vector/matrix formulations. The Drucker-Prager criterion is introduced together with Wu-Tanabe's damage-based model as a well-refined constitutive representation. Numerical simulations are made for nonlinear behavior and detection of failure modes of confined concrete. The discussion of diffuse failure vs. localized failure for concrete as well as yield condition for lateral reinforcement is also made.

Introduction

It has been known that concrete exhibits spatial discontinuities in the form

[1] Dept. of Civil Engrg., Musashi Inst. of Tech., Tokyo, Japan.
[2] Construction Management Office, Nippon Koei Co., Ltd., Tokyo, Japan

of localization as well as diffuse failure. In this paper, the inelastic analysis of concrete confined by the lateral reinforcement or steel jacket is presented. As a typical structural member in which concrete is in a compressive triaxial stress state, we here consider a simplified tied column or a steel encased column under a uniaxial compressive force. Ultimate strengths and ductility are enhanced by the mechanical confinement provided by the lateral reinforcement or steel jacket. Then, we develop a macroscopic model rather than a discretized technique such as a finite element analysis for a rectangular reinforced concrete column.

Numerical simulation is carried out using the Drucker-Prager model. Detection of failure modes of confined concrete is also made: diffuse failure vs. localized failure for concrete as well as yield condition for lateral reinforcement are analyzed. The diffuse failure corresponding to C^1-continuity can be detected by the singularity of tangential constitutive stiffness, while the localized failure in C^0-continuity can be identified by the singularity of localization tensor. The present analytical investigation is a fundamental discussion for concrete in triaxial compressive stresses through the idealized confined concrete.

Analytical Model of Confined Concrete

In order to simplify the present problem, stresses and strains are assumed to be uniform in the longitudinal direction and throughout the section shown in Figure 1. The core concrete in a column is only considered, while the cover concrete is neglected for the analytical model. Therefore, we can deal with this problem as a pointwise-argument on the constitutive level.

Let the stress vector of concrete be $\{\sigma_{ij}^c\}$ and the lateral reinforcement $\{\sigma_i^s\}$, and likewise the strain vector for concrete $\{\varepsilon_{ij}^c\}$ and the strain vector for reinforcement $\{\varepsilon_{ij}^s\}$. With the application of an axial compressive force denoted by $\sigma_{33} < 0$, all stress vectors are related to each other as the equilibrium condition in the rate form such that,

$$\left[0 \quad 0 \quad \dot{\sigma}_{33}\right]^T = \left[\dot{\sigma}_{11}^c \quad \dot{\sigma}_{22}^c \quad \dot{\sigma}_{33}^c\right]^T + p\left[\dot{\sigma}_1^s \quad \dot{\sigma}_2^s \quad 0\right]^T \tag{1}$$

where p expresses the sectional ratio of lateral reinforcement in the 1-direction and 2-direction. The superscript c indicates concrete and s reinforcing steel, and 1, 2, and 3 mean the directions shown in Figure 1. It is obvious that the tensile stresses in the lateral ties and the compressive stresses of the confined reaction to the lateral ties are balanced in the transverse directions 1 and 2.

Because the confined concrete and the lateral reinforcement are assumed to be deformed identically, the strain vectors of concrete and reinforcement are compatible with the total strain, being simply expressed as follows.

$$\{\dot{\varepsilon}\} = \{\dot{\varepsilon}_c\} = \{\dot{\varepsilon}_s\} \tag{2}$$

Next, the tangential stiffness of concrete and that of reinforcement in the matrix form are introduced, then the constitutive relationships result in,

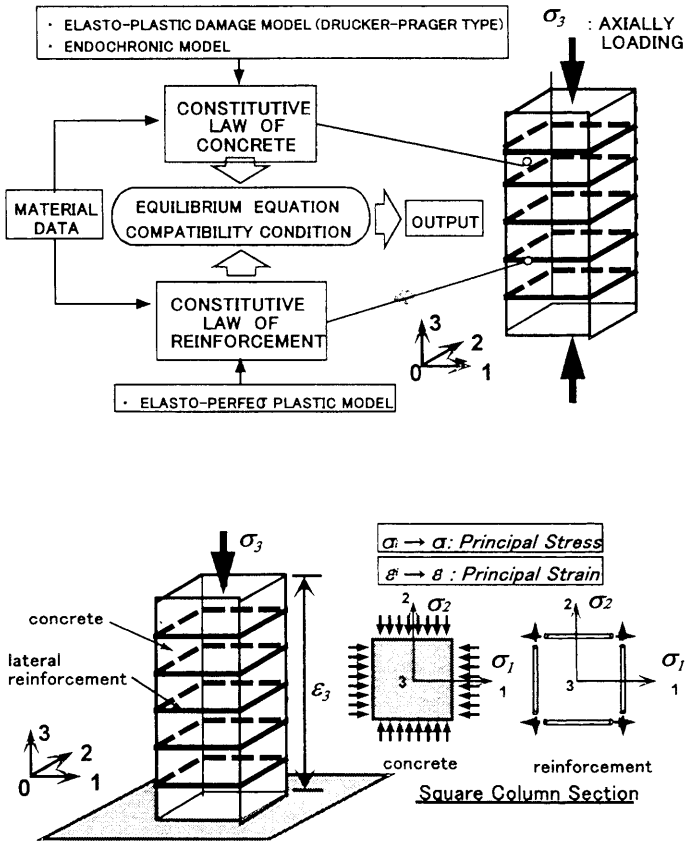

Figure 1. Analytical Modeling of Confined Concrete and Lateral Reinforcement

$$\begin{bmatrix} \dot{\sigma}^c_{11} \\ \dot{\sigma}^c_{22} \\ \dot{\sigma}^c_{33} \end{bmatrix} = \begin{bmatrix} D^{ep}_{1111} & D^{ep}_{1122} & D^{ep}_{1133} \\ D^{ep}_{2211} & D^{ep}_{2222} & D^{ep}_{2233} \\ D^{ep}_{3311} & D^{ep}_{3322} & D^{ep}_{3333} \end{bmatrix} \begin{bmatrix} \dot{\varepsilon}_{11} \\ \dot{\varepsilon}_{22} \\ \dot{\varepsilon}_{33} \end{bmatrix} \tag{3}$$

$$\begin{bmatrix} \dot{\sigma}^s_1 \\ \dot{\sigma}^s_2 \\ 0 \end{bmatrix} = \begin{bmatrix} E_s & 0 & 0 \\ & E_s & 0 \\ sym. & & 0 \end{bmatrix} \begin{bmatrix} \dot{\varepsilon}_{11} \\ \dot{\varepsilon}_{22} \\ \dot{\varepsilon}_{33} \end{bmatrix} \tag{4}$$

In which, the concrete constitutive matrix $[\, D^{ep}_{ijkl} \,]$ defines the isotropic elasto-plastic softening behavior and the lateral reinforcement is assumed to be simply the elasto perfect-plastic two ways system. Furthermore, a right square section of a column is considered here, and the section can be reduced to a transversely isotropic solid such that $\sigma^c_{11} = \sigma^c_{22}$, $\sigma^s_1 = \sigma^s_2$, and $\varepsilon_{11} = \varepsilon_{22}$.

By arranging the equilibrium condition by Eq. (1) and the compatibility condition by Eq. (2) together with the Eqs. (3) and (4), then the following representations can be formulated.

$$\dot{\varepsilon}_{11} = \dot{\varepsilon}_{22} = \frac{-D^{ep}_{1133}}{D^{ep}_{1111} + D^{ep}_{1122} + pE_s} \dot{\varepsilon}_{33} = \frac{-D^{ep}_{2233}}{D^{ep}_{2211} + D^{ep}_{2222} + pE_s} \dot{\varepsilon}_{33} \tag{5}$$

$$\dot{\sigma}_{33} = \left[D^{ep}_{3333} - \frac{D^{ep}_{1133}\left(D^{ep}_{3311} + D^{ep}_{3322}\right)}{D^{ep}_{1111} + D^{ep}_{1122} + pE_s} \right] \dot{\varepsilon}_{33} = \left[D^{ep}_{3333} - \frac{D^{ep}_{2233}\left(D^{ep}_{3311} + D^{ep}_{3322}\right)}{D^{ep}_{2211} + D^{ep}_{2222} + pE_s} \right] \dot{\varepsilon}_{33} \tag{6}$$

With regard to the stiffness of lateral reinforcement, whichever the reinforcing bars or the steel casing, the degree of confining effect is simply represented by pE_s which appears in the formulated equations.

Eq. (5) implies that the lateral strains ε_{11} , ε_{22} swell due to the compressive strain $\varepsilon_{33} (< 0)$, being inversely proportional to the degree of confinement expressed by pEs. If an apparent value of the Poisson's ratio of confined concrete is defined such that $\nu^* \equiv -\dot{\varepsilon}_{11} / \dot{\varepsilon}_{33} = -\dot{\varepsilon}_{22} / \dot{\varepsilon}_{33}$, this is calculated as

$$\nu^* = \frac{D^{ep}_{1133}}{D^{ep}_{1111} + D^{ep}_{1122} + pE_s} = \frac{D^{ep}_{2233}}{D^{ep}_{2211} + D^{ep}_{2222} + pE_s} \tag{7}$$

Finally, the concrete stresses σ_{11}^{c} and σ_{22}^{c} in the lateral direction and σ_{33}^{c} in the longitudinal direction as well as the stresses of lateral reinforcement σ_{1}^{s} and σ_{2}^{s} are obtained as follows.

$$\dot{\sigma}_{11}^{c} = \dot{\sigma}_{22}^{c} = \left[D_{1133}^{ep} - \frac{D_{1133}^{ep}\left(D_{1111}^{ep} + D_{1122}^{ep}\right)}{D_{1111}^{ep} + D_{1122}^{ep} + pE_{s}} \right] \dot{\varepsilon}_{33} \tag{8}$$

$$\dot{\sigma}_{33}^{c} = \dot{\sigma}_{33} = \left[D_{3333}^{ep} - \frac{D_{1133}^{ep}\left(D_{3311}^{ep} + D_{3322}^{ep}\right)}{D_{1111}^{ep} + D_{1122}^{ep} + pE_{s}} \right] \dot{\varepsilon}_{33} = \left[D_{3333}^{ep} - \frac{D_{2233}^{ep}\left(D_{3311}^{ep} + D_{3322}^{ep}\right)}{D_{2211}^{ep} + D_{2222}^{ep} + pE_{s}} \right] \dot{\varepsilon}_{33} \tag{9}$$

$$\dot{\sigma}_{1}^{s} = \dot{\sigma}_{2}^{s} = \frac{-D_{1133}^{ep}}{D_{1111}^{ep} + D_{1122}^{ep} + pE_{s}} \dot{\varepsilon}_{33} E_{s} \tag{10}$$

It is found that when $\varepsilon_{33} < 0$, the concrete stresses in the lateral direction turn out to be compression while the reinforcement become tension ties, and that those stresses are balanced as the action and reaction forces. It should be noted that the member in consideration becomes unconfined concrete such that $\sigma_{11}^{c} = \sigma_{22}^{c} = 0$ when $pE_s = 0$, and a perfectly constrained concrete such that $\varepsilon_{11} = \varepsilon_{22} = 0$ when $pE_s = \infty$.

Elasto-Plastic Damage Model

Drucker-Prager Model

Here in this study, we employed the non-associated elasto-plastic constitutive model of the tangential operator in the form

$$\dot{\sigma}_{ij}^{c} = D_{ijkl}^{ep} \dot{\varepsilon}_{kl}^{c}, \quad D_{ijkl}^{ep} = E_{ijkl}^{e} - E_{ijkl}^{p} \quad (i, j, k, l = 1, 2, 3) \tag{11}$$

This forth-order constitutive tensor is comprised of the elastic stiffness E_{ijkl}^{e} and the rank one modification E_{ijkl}^{p} due to plasticity, which are expressed as

$$E_{ijkl}^{e} = \frac{E}{1+\nu}\left\{ \frac{\nu}{1-2\nu}\delta_{ij}\delta_{kl} + \frac{1}{2}\left(\delta_{ik}\delta_{jl} + \delta_{il}\delta_{jk}\right) \right\} \tag{12}$$

$$E_{ijkl}^{p} = \frac{E_{ijmn}^{e} m_{mn} n_{pq} E_{pqkl}^{e}}{H_{p} + n_{mn} E_{mnpq}^{e} m_{pq}} \tag{13}$$

where E and ν are elastic material constants, and the scalar quantity H_p defines the plastic modulus. The two gradient directions are given as

$$n_{ij} = \frac{\partial f}{\partial \sigma_{ij}} \quad , \quad m_{ij} = \frac{\partial q}{\partial \sigma_{ij}} \tag{14}$$

The Drucker-Prager model is introduced for the yield criterion f and the plastic potential q in the form

$$f = \alpha I_1 + \sqrt{J_2} - k = 0 \quad , \quad q = \beta I_1 + \sqrt{J_2} - k' = 0 \tag{15}$$

The Drucker-Pager format includes the first invariant of stress tensor I_1 and the second invariant of deviatoric stress tensor J_2. It is also known that for $\alpha \neq \beta$ we have a non-associated flow rule and for $\alpha = \beta$ we have an associated flow rule, and that in the case of $\alpha = \beta = 0$, the Drucker–Prager model reduces to the von-Mises criterion.

Wu-Tanabe's Damage Model

In order to represent the hardening and softening behavior of quasi-brittle materials like concrete in compression, we introduced the damage-based model proposed by Wu and Tanabe (1990). This model resorts to converting the Drucker–Prager model expression to the Mohr-Coulomb hexagonal surface by the compressive meridian matching through

$$\alpha = \frac{2\sin\phi_f}{\sqrt{3}(3-\sin\phi_f)} \quad , \quad k = \frac{6c\cos\phi_f}{\sqrt{3}(3-\sin\phi_f)} \tag{16}$$

The cohesion c and the internal friction angle ϕ used for the yield criterion are given by

$$c = c_0 \exp\left[-(m\omega)^2\right] \tag{17}$$

$$\phi_f = \begin{cases} \phi_0\sqrt{2\omega - \omega^2} & : \ \omega \leq 1 \\ \phi_0 & : \ \omega > 1 \end{cases} \tag{18}$$

in which m is the material constant, c_0 and ϕ_0 are the initial values, and ω is the isotropic damage index, which is calculated by means of the plastic work.

Likewise to the plastic potential q for the conversion to the Mohr-Coulomb format and parameters expression are given such that

$$\beta = \frac{2\sin\psi_f}{\sqrt{3}(3-\sin\psi_f)} \quad , \quad k' = \frac{6c\cos\psi_f}{\sqrt{3}(3-\sin\psi_f)} \tag{19}$$

where c is the cohesion again and ψ_f the dilatancy angle that is given by

$$\psi_f = \begin{cases} \psi_0\sqrt{2\omega-\omega^2} & : \ \omega \le 1 \\ \psi_0 & : \ \omega > 1 \end{cases} \tag{20}$$

in which ψ_0 is the initial value of dilatancy angle, and ω is again the isotropic damage index.

In actual calculations for this isotropic elasto-plastic damage model, the plastic potential q is figured out by $\beta = \Delta\alpha$ (where Δ is the non-associativeness factor). By setting $\Delta = 1$, we have an associated flow rule, whereas when $0 < \Delta < 1$, we have a non-associated flow rule and for $\Delta = 0$, the plastic potential q reduces to the von-Mises criterion as a special case.

Note that the material parameters such as the cohesion c, the internal friction angle ϕ and the dilation angle φ evolve, depending on the damage accumulated with the plastic work ω. Figure 2 draws the variation of major parameters and damage evolution, and the resulting stress~strain relations, where a material constant χ was changed as a parameter. It is observed in this figure that the cohesion c decreases and the internal friction angle ϕ increases with the increase of the isotropic damage index ω and realistic curves for the stress~strain relation are reproduced.

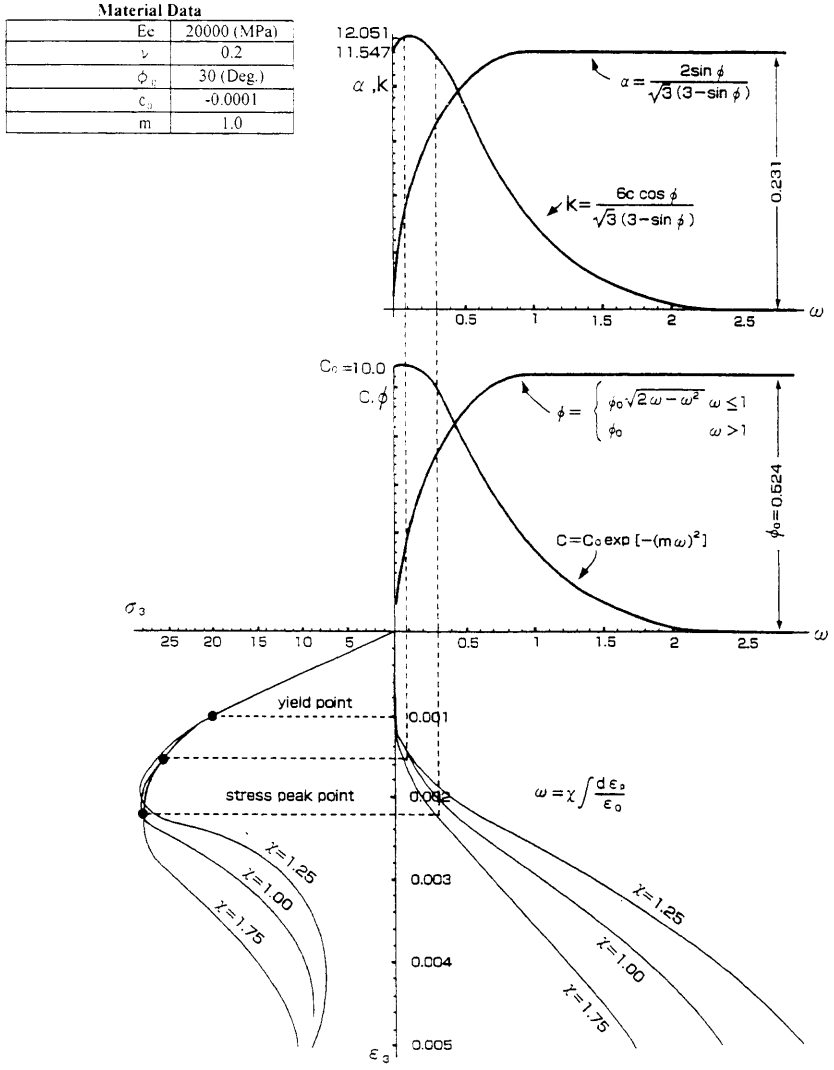

Figure 2. Elasto-Plastic Damage Model:
Variation of Parameters and Stress~Strain Relation

Parameter Determination

Numerical Examples for the uniaxial compression are shown in Figure 3. In the figure, the influence of the material parameters on the uniaxial behavior is examined in comparison with the conventional formulas from Popovics (1972) and CEB-FIP Model Code (1990). The set of five material parameters listed in Figure 3 is determined by fitting the uniaxial stress~strain relation to the CEB-FIP model curve, which will be used in subsequent computations. Furthermore, the more wide-range of parametric simulations by Yamakawa (1996) indicated that when the larger c_0, ϕ_0 and t_0, the smaller χ_0, then the larger the ultimate strength and the corresponding strains are available.

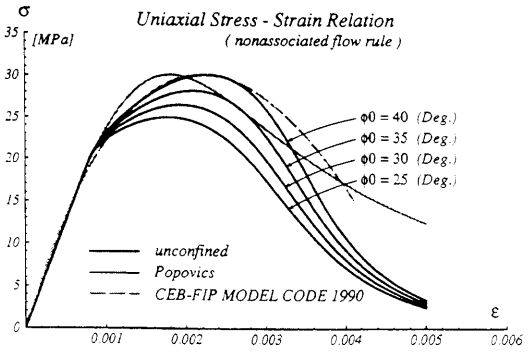

Material Data	
Ec	25000 (MPa)
Es	210000 (MPa)
ν	0.2
d ε_0	-0.0001
p	0.0 (unconfined)
ϕ_0	variable (Deg.)
c_0	10.0 (MPa)
ε_0	0.002
χ_0	0.65
m_0	1.0
Δ	0.0 (nonassociativeness)

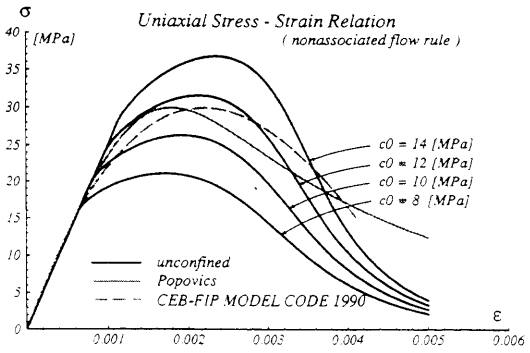

Material Data	
Ec	25000 (MPa)
Es	210000 (MPa)
ν	0.2
d ε_0	-0.0001
p	0.0 (unconfined)
ϕ_0	30.0 (Deg.)
c_0	variable (MPa)
ε_0	0.002
χ_0	0.65
m_0	1.0
Δ	0.0 (nonassociativeness)

Figure 3. Uniaxial Stress~Strain Relation in Comparison with Conventional Formulas

Numerical Simulation of Confined Concrete

Shown in Figure 4 are numerical results of the proposed model for the confined concrete where the reinforcement ratio p=0~2% is chosen as a parameter. The upper figure is obtained based on the elasto-plastic damage model (the non-associated/associated flow rule), while the lower ones are based on the Endochronic model proposed by Bazant, et al. (1976), which is employed as an alternative constitutive law. It is assumed that $\alpha \neq 0$ and $\beta = 0$ for the non-associated flow rule while $\alpha = \beta$ for the associated flow rule. It is found that with the increase of the lateral reinforcement, the strength and strains were enhanced and an obvious confining effect was observed.

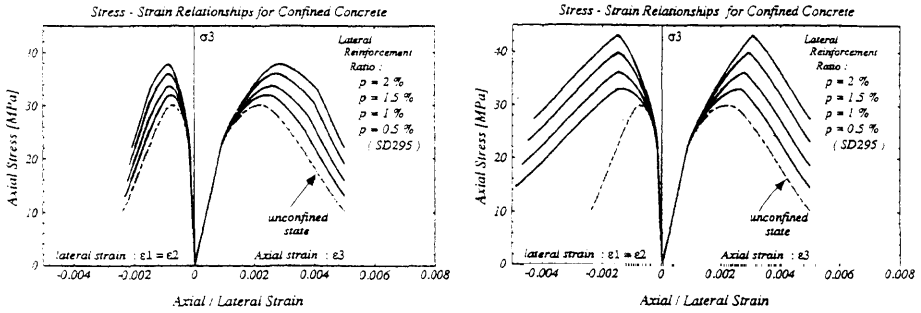

Figure 4(a). Nonlinear Behavior of Confined Concrete by Elasto-Plastic Damage Model (left: Non-Associated Flow Rule, right: Associated Flow Rule)

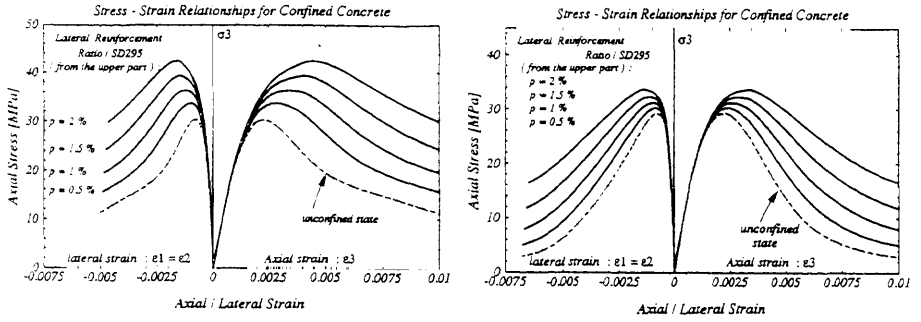

(Type-I) (Type-III)

Figure 4(b). Nonlinear Behavior of Confined Concrete by Endochronic Model (left: Type Ⅰ, right: TypeⅢ)

Figure 5 depicts nonlinear behavior of the confined concrete and the lateral reinforcement, where points of the ultimate concrete strength and the yielding of reinforcement are marked. Note that in all cases in the figures, the yielding of lateral reinforcement took place after the stress peak point of concrete, i.e., on the

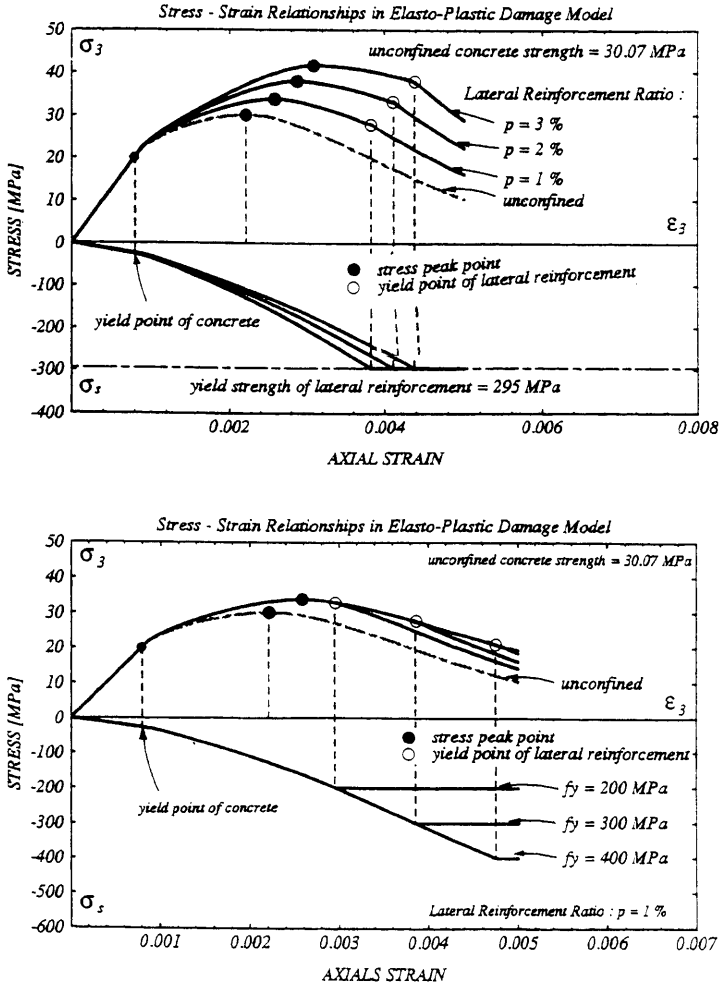

Figure 5. Nonlinear Behavior of Lateral Reinforcement and Confined Concrete Parameter:Lateral Reinforcement Ratios (upper), Parameter: Yield Strengths (lower)

descending branch of stress~strain curve of concrete which coincides with a suggestion in Irawan and Maekawa (1993). However, according to the further investigation (Yamakawa (1998)), the reinforcement yielded prior to the stress peak point of the concrete when the Endochronic theory was utilized. This implies that it depends not only on the degree of mechanical confinement, but also on the characteristics of the constitutive law whether the lateral reinforcement yields before or after the stress peak point.

Next, in order to examine how much the ultimate strength and strain are improved by means of the confining reinforcement, we define the following indices.

$$\eta^* = f_c^* / f_c' \tag{21}$$

$$\xi^* = \varepsilon_c^* / \varepsilon_c' \tag{22}$$

in which f_c' and ε_c' are the ultimate strength and the strain at the stress peak point for unconfined concrete, respectively, and f_c^*, ε_c^* are those for confined concrete.

Shown in Figure 6 are these enhancement indices in relation to confinement level expressed by pf_y. It is found that the strengths and the strains linearly increase in proportion to the reinforcement content pf_y. In this figure, numerical results by means of (a) non-associated elasto-plastic damage model and (b) Endochronic model Type II were shown in comparison of design formulas by JRA Specification (1996) and Kent and Park. (1971).

These figures imply that with regard to strength enhancement the calculated values and predictions by JRA Specification (1996) and Kent and Park. (1971) almost coincide, whereas there are large differences in the increase of strains among the calculated values and predicted values by these two formulas.

Diagnostics of Concrete Failures

Failure Description

A discussion of failure mechanisms at the material level inevitably concerns three distinctly separate modes: diffuse failure, localized failure and discrete failure (Willam, et al. (1995)). This categorization is based on the degree of C-continuity; spacious discontinuity of the kinematic fields. Among the three aforementioned modes, we here deal with the first two, addressed as follows.

Diffuse failure corresponds to C^1-continuity, which underlies the singularity of the tangential material operator. This implies the classic instability argument in the small signals through the vanishing values of the second order work density in the form

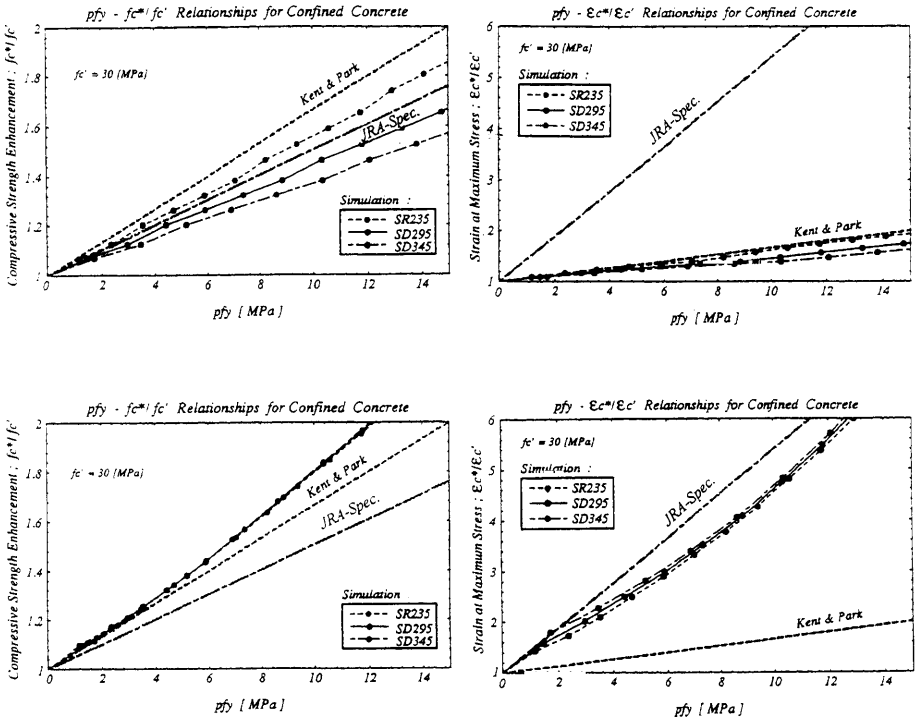

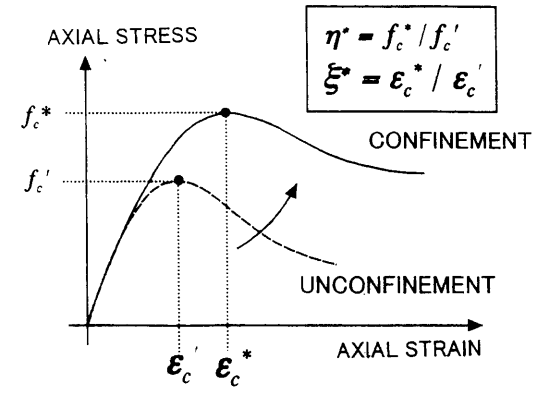

Figure 6. Enhancement of Concrete Properties due to Confinement:
(a) Non-associated Elasto-Plastic Damage Model, (b) Endochronic Model Type II
(left: Maximum Strength of Concrete, right: Strain at Maximum Strength)

$$d^2W = \dot{\boldsymbol{\varepsilon}} : \dot{\boldsymbol{\sigma}} = \dot{\boldsymbol{\varepsilon}} : \mathbf{D}_{ep} : \dot{\boldsymbol{\varepsilon}} = 0 \tag{23}$$

An alternative criterion for the diffuse failure is provided as the singularity of the tangential operator in the form

$$det(\mathbf{D}_{ep}) = 0 \tag{24}$$

It has been pointed out that when the symmetric constitutive operator is adopted, both of the above criteria lead to the same consequences, while in the case of the non-symmetric operator like the non-associated flow, these criteria don't coincide resulting in $d^2W \le det(\mathbf{D}_{ep})$.

Localized failure corresponds to C^0-continuity, which means that the singularity of the localization tensor signals the formation of the spatial discontinuity. This is

$$det(\mathbf{Q}_{ep}) = 0, \ \mathbf{Q}_{ep} = \mathbf{N} \cdot \mathbf{D}_{ep} \cdot \mathbf{N} \tag{25}$$

Alternatively, the localization argument for discontinuous bifurcation can be expressed in terms of a quadratic form

$$\dot{\gamma} = \rho c^2 = \mathbf{M} \cdot \mathbf{Q}_{ep} \cdot \mathbf{M} = (\mathbf{M} \otimes \mathbf{N}) : \mathbf{D}_{ep} : (\mathbf{N} \otimes \mathbf{M}) = 0 \tag{26}$$

Two directional unit-vectors are defined as $\mathbf{N}$: the orientation of discontinuity surface and $\mathbf{M}$: direction of the localized motion. These fundamental descriptions are well explained in, for examples, Runesson et al. (1991).

Numerical Demonstration of Failure Diagnosis

Then, we define the following two indicators to detect the onset of the diffuse/localized failures.

$$\eta^{dif} = det(\mathbf{D}_{ep}) / det(\mathbf{D}_e), \text{ or } \eta^{dif} = d^2W_{ep} / d^2W_e \tag{27}$$

$$\lambda^{loc} = det(\mathbf{Q}_{ep}) / det(\mathbf{Q}_e) \tag{28}$$

The indicator η^{dif} is regarded as the first eigenvalue of the tangential operator $\mathbf{D}_{ep}$ normalized with respect to the elastic part $\mathbf{E}_e$. The indicator λ^{loc} is the eigenvalue of the characteristic tensor of localization $\mathbf{Q}_e$ normalized by its elastic counterpart $\mathbf{Q}_e$, where $\mathbf{Q}_e = \mathbf{N} \cdot \mathbf{E}_e \cdot \mathbf{N}$. These two normalized indices range from 1

to 0, depending on their plasticity, and signal the onset of diffuse or localized failure such that:

$$\begin{array}{ll} \text{elastic stage} & : \eta^{dif} = 1,\ \lambda^{loc} = 1 \\ \text{plastic stage} & : 0 < \eta^{dif} < 1,\ 0 < \lambda^{loc} < 1 \\ \text{diffuse failure} & : \eta^{dif} = 0 \\ \text{localized failure} & : \lambda^{loc} = 0 \end{array} \tag{29}$$

The mathematical formulation through the eigen-analysis for the localized failure may be referred to in Yoshikawa et al. (1993).

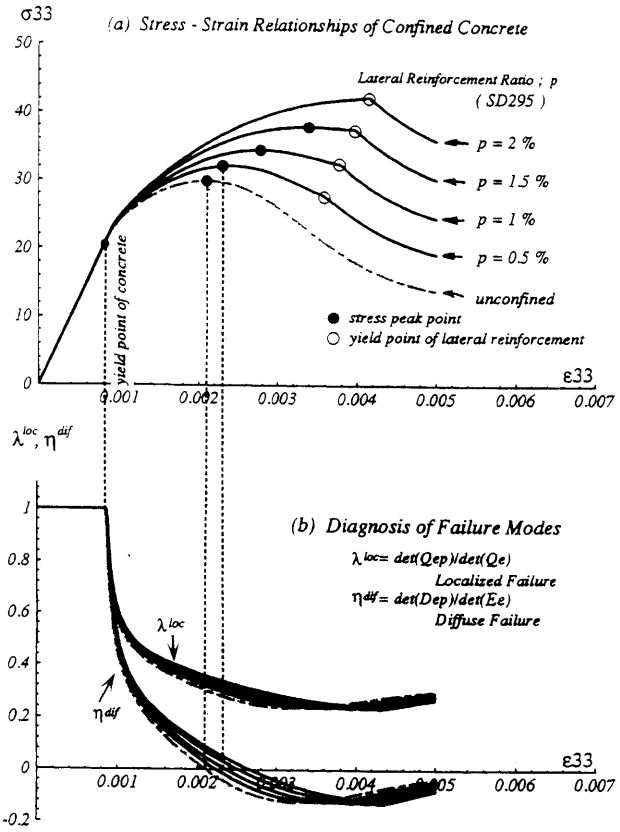

Figure 7. Diagnosis of Concrete Failure Modes: Stress~Strain Relation and Mode Indices

Figure 7 shows the stress~strain relation of confined concrete (upper part) and the variation of the two indicators η^{dis} and λ^{loc} (lower part). Both indicators maintained 1 until the initial yielding of concrete and then decreased during the plastic state. The important feature is that η^{dis} came to be 0 while λ^{loc} remained positive, for all cases in Figure 7 regardless of the amount of lateral reinforcement, which implies the diffuse failure was initiated first.

Apart from these computations for confined concrete, we carried out another numerical calculation for plain concrete subjected to proportional biaxial/triaxial loading by strain control again based on the elasto-plastic damage model. Figure 8 illustrates the results of failure identification in the $r-\xi$ coordinates, where these two notations are

$$r=\sqrt{2J_2}\ ,\ \xi=I_1/\sqrt{3} \tag{30}$$

This figure indicated that localization failure is detected prior to diffuse failure only in the higher hydrostatic stress region.

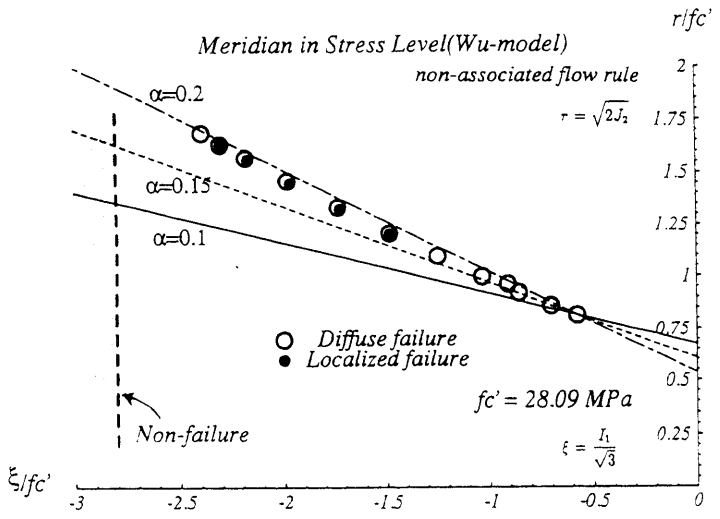

Figure 8. Identification of Failure Modes expressed in the $r-\xi$ coordinates

The tendency concerning failure mechanisms (diffuse failure vs. localized failure) depends, of course, on the constitutive expression used. From a mathematical point of view, solid in the triaxial stress state appears to be less susceptible to the localization compared to one in the plane stress state as is often pointed out. It may be suggested that the lower volumetric compressive pressure causes diffuse failure, and the higher pressure leads to localized failure, which was mentioned in experiments by van Mier (1986) and in numerical consideration in Shizuma and Yoshikawa (1997).

The Drucker-Pager format includes the first invariant of stress tensor I_1 and the second invariant of deviatoric stress tensor J_2, lacking the third invariant of deviator stress tensor J_3. It is supposed that inclusion of this invariant J_3 may provide different numerical results leading to more realistic consequences.

Concluding Remarks

The present paper is a fundamental study for concrete in the triaxial stress-state through the idealized confined concrete in order to investigate nonlinear deformational behavior and failure-detection characteristics. By means of construction of macroscopic modeling for confined concrete, we can deal with this issue on the stress/strain level.

Through the various numerical simulations, nonlinear behavior and failure modes of concrete were observed. It was found that non-associated elasto-plastic model incorporating the Drucker-Prager criterion together with Wu-Tanabe's damage-based hardening rule can reproduce the realistic behavior of confined concrete. It may be concluded that property and usefulness of constitutive representation should be examined not only by its deformational behavior in a biaxial/triaxial stress state, but also by its capability of failure mode identification.

Detection of localization and analysis of bifurcated material are really essential keys of inelasticity of quasi-brittle materials. Therefore, strain localization as a bifurcation problem needs be taken into consideration to examine the characteristics of constitutive model. As recent examples of post-bifurcation analysis, Yoshikawa, Nagano and Willam (1995) and Shizuma and Yoshikawa (1998) may be referred to. Through the eigenanalyses of the localization tensor as well as the tangent operator which are still argued at the material level, we can observe fundamental aspects of constitutive models (Yoshikawa and Willam (1993)).

References

Bazant, Z.P. and Bahat, P.D. (1976). "Endochronic theory of inelasticity and failure of concrete." *Journal of the Engineering Mechanics Division,* ASCE, 102(EM4), 701-722.

Comite Euro-International Du Beton (1996). *CEB-FIP Model Code (1990), Design Code,* Thomas Telford.

Irawan, P. and Maekawa, K. (1993). "Strength and damage analysis of concrete confined by steel casing." *Journal of Materials, Concrete Structures and Pavements,* JSCE, N0.472/V-20, 97-106. (in Japanese)

Japan Road Association (1996). *Specification for Highway Bridges,* Part V: Earthquake-resistant design, Chapter 9. (in Japanese)

Kent, D.C. and Park, R. (1971). "Flexural members with confined concrete." *Journal of the Structural Division,* ASCE, 97(ST7), 1969-1990.

van Mier, J.G.M. (1986). "Multiaxial strain-softening of concrete, Part I: Fracture, Part 2: Load Histories." *Materials and Structures,* RILEM, 19(111), 179-200.

Popovics, S. (1973). "A numerical approach to the complete stress-strain curve of concrete." *Cement and Concrete Research,* 3(5), 583-559.

Runesson, K., Ottosen, N.S., and Peric, D. (1991). "Discontinuous bifurcation of elasto-plastic solutions in plane stress and plane strain." *International Journal of Plasticity,* 7, 99-121 .

Shizuma, T., and Yoshikawa, H. (1998). "Non-linear behavior and diagnosis of failure modes of quasi-brittle materials under multiaxial loading conditions." *Concrete Research and Technology,* JCI, 9-1, 99-112. (in Japanese)

Willam, K., Etse, G., and Munz, T. (1994). "Localized failure in elastic-viscoplastic materials." Drafted Research Report, CEAE-Department, Univ. of Colorado at Boulder.

Wu, Z., and Tanabe, T. (1990). "A hardening/softening model of concrete subjected to compressive loading." *Journal of Structural Engineering,* AIJ, 36B, 153-162.

Yamakawa, K. (1998). *Analytical Study of Strain Localization in Quasibrittle Materials under Multiaxial Loading Condition,* Master Degree Thesis, Musashi Institute of Technology, Research Division in Engineering. (in Japanese)

Yoshikawa, H. (1993). *Fundamental Study on Strain Localization as Bifurcation Problem for Elasto-Plastic Materials*, Research Report, CEAE-Department, Univ. of Colorado at Boulder.

Yoshikawa, H. and Willam, K. (1993). "Analysis of localized failure in elasto-plastic solids." *Fracture of Brittle, Disordered Materials: Concrete, Rock and Ceramics,* E&FN SPON, IUTAM, 464-478.

Yoshikawa, H., Nagano, R., and Willam, K. (1995). "Strain localization as bifurcation of elasto-plastic softening materials." *Fracture Mechanics of Concrete Structures,* FRAMCOS-2, 2, 1079-1088.